



American Journal of Innovation in Science and Engineering (AJISE)

ISSN: 2158-7205 (ONLINE)

VOLUME 5 ISSUE 1 (2026)



PUBLISHED BY
E-PALLI PUBLISHERS, DELAWARE, USA

Environmentally Friendly Synthesis of Hierarchical Porous Activated Carbon From Biomass Waste for Enhanced Supercapacitor Performance and Measured by Voltage Holding Method

T. E Amakoromo^{1*}, P. S. Cooney²

Article Information

Received: November 02, 2025

Accepted: March 13, 2026

Published: April 20, 2026

Keywords

Biomass, Stability Charge Storage, Super Capacitor, Voltage-Holding Method

ABSTRACT

Supercapacitors remain highly efficient energy storage devices, which rely on electrochemical processes, however, stability over extended periods remains a major concern. In this study, the performance of a biomass-derived device is tested using the voltage holding method. The device exhibited a specific capacitance of 55Fg⁻¹ at 0.5Ag⁻¹ and a maximum energy density of 8.14Whkg⁻¹ at 250Wkg⁻¹ power density. Consequently, a 10h floating period was followed by consecutive constant current charge discharge (CCCD) cycles to identify any capacitance loss over a 72 h (3days) period. It was observed that within the first 50 h, there was no noticeable loss in capacitance which shows high stability at the set voltage of 1.6V and time window. However, beyond 50 hours of exposure and running up to 72 h, a capacitance loss of 44% was observed. This voltage holding method tells the true story of the stability patterns of supercapacitors as it gives insight via an aggressive aging process.

INTRODUCTION

Non-renewable resource consumption will undoubtedly have major environmental implications, because of the rate of consumptions, we must swiftly transition to greener, more sustainable types of energy production. Nonetheless, this transition is challenged by the intermittent nature of renewable energy sources, as well as their scarcity (Li *et al.*, 2022; Mutuma *et al.*, 2021)

These obstacles will be easier to overcome if efforts are focused on discovering, developing, and improving renewable energy storage systems. Supercapacitors have sparked considerable interest among other energy storage technologies. They have advantages over alternatives such as batteries and fuel cells due to their unique properties. These features include a fast charge-up time, a high cycle life, and a fast charge-discharge rate. They are also superior to other techniques of data storage in terms of environmental impact [Large-scale single-step synthesis of wrinkled N-S doped 3D graphene like nanosheets from Tender palm shoots for high energy density supercapacitors.

The advent of electric vehicles, coupled with continuous miniaturization of electronic devices, efficient energy storage systems have become very important. Batteries have long played this role but for their poor power densities, reliance is now shifted to the supercapacitors. Typical supercapacitors include electric double-layer capacitors (EDLC), pseudocapacitors (PC), and battery-type capacitors (BT). Electrode materials utilized in EDLCs store energy by separating charges at the electrolyte-electrode interface and benefit from extremely high

specific surface areas, broad working potential windows, and high electrical conductivities. These characteristics result in high specific power and rapid discharge. Rapid redox processes at the electrolyte/electrode interface provide PC and BT with high theoretical specific capacities and specific energies (Elgendy *et al.*, 2020; Jo *et al.*, 2022) EDLC electrodes can be easily made from activated carbon (AC) and this has opened up another broad research area to not only make the activated carbon produced for this purpose environmentally friendly, but also very cheap and readily available. The catch in this interest is the porosity, good electrical conductivity and electrical stability of activated carbon and the high carbon content which is suitable for energy storage. The performance of supercapacitors is significantly impacted by two important parameters: electrodes and electrolytes. Improving our knowledge of nanoscale surfaces and their electrochemical characteristics is a promising route for improving SC's performance. This will increase the device's specific energy while taking advantage of its very high specific power.

EDLCs stores energy in the interfacial region between the electrolyte and a carbon material with high surface area under applied cell voltage. In this system, no chemical reactions occur, hence the process of charge storage is considered to be predominantly physical, which contributes majorly to the excellent recyclability of these types of supercapacitors, as degradation during the charge-discharge process occurs at an almost insignificant rate. In contrast, the other popular type of supercapacitors pseudocapacitors and hybrid supercapacitors utilize

¹ Department of Physics/Electronics Technology, University of Port Harcourt, Rivers State, Nigeria

² Department of Physics/Electronics Technology, Federal Polytechnic of Oil and Gas, Bonny, Rivers State, Nigeria.

* Corresponding author's e-mail: tarila.amakoromo@uniport.edu.ng

faradaic redox process in its charge storage mechanism. In this type of devices, storage of charges involves chemical reactions between ions from the electrolytes and interactions with the bulk of electrode materials and as a result, higher specific capacitance values have been reported from such devices in comparison with the EDLC device. However, as the charge and discharge process continues over time, degradation of the bulk material and the electrolyte is observed which reduces the chemical stability of the device. Pseudocapacitors therefore, despite showing higher capacitance values than EDLCs still lack commercial adoption due to high cost and poor chemical cycling stability (Noori *et al.*, 2019). Materials with a hierarchical pore size distribution (micropores, mesopores, and macropores), a high specific surface area, and strong electrical conductivity are frequently used to fabricate EDLCs. Several carbon-based materials, including graphene, activated carbon (AC), carbon aerogels, and carbon nanotubes, share these properties. Activated carbon is an excellent electrode material for supercapacitors due to its large specific surface area and pore volume. Furthermore, activated carbon has advantages including a high adsorption capacity, chemical stability, ordered porous architectures, and low production costs. It is easily produced from biomass since it is abundant, renewable, non-toxic, and does not disorient the environment. It is produced by a multi-step process that begins with pyrolysis and culminates in high-temperature, oxygen-free activation processes. Chemical diversity in biomass can also be exploited to create capacitive materials with supercapacitor-relevant properties.

Using easily assessable biomass as starting materials will prove cost effective and show availability at all times, and to scale up the production of activated carbon from biomass precursors on a large scale, research in this field should focus on developing dependable yet easy approaches. Numerous studies have shown that activated carbon derived from various sources, including tree bark biomass, sugarcane bagasse, bamboo, banana, cassava, orange, capsicum, coconut, peanut, and bamboo, olive stones, niral palm nut, corncob, rice husk and hydrochar amarula seed husk, improves electrochemical performance.

Potassium hydroxide KOH has become the preferred activating agent in chemical activation of biomass for production of carbon materials with high porosity. However, industrial adoption of this method of activation is still low due to the environmental challenges it comes with because of its corrosive nature (Sevilla & Fuertes, 2016). Attempts have been made in the past to use sodium salts as an alternative activating agent due to its environmental friendliness and non-corrosive attributes, however the yielded materials showed poor surface properties making it less attractive to potassium salts. For instance, poor BET surface area value of 552m²g⁻¹ for big bluestem activated with sodium bicarbonate (Jin *et al.*, 2014) has been reported. Other

activating agents like ZnCl₂ has also gained lots of popularity in producing porous carbons for applications in the supercapacitor space (Electrochemical Capacitive Performance of ZnCl₂ Activated Carbon Derived from Bamboo Bagasse in Aqueous and Organic Electrolyte: Oriental Journal of Chemistry, n.d.) (Zhu *et al.*, 2020), however it is also reportedly very corrosive and toxic in nature (ZINC Chloride | ZnCl₂ - PubChem, n.d.), hence its wide adoption is also hampered.

One characteristic that makes EDLCs to stand out is their cycle stability. Stability studies around supercapacitors are traditionally demonstrated by cycling the new device for several thousands of cycles using cyclic voltammetry by implementing a constant current charge-discharge (CCCD), which leaves the device with a not so significant loss of capacitance after the cycles (Bello *et al.*, 2016). This method of determining the stability of the device is time consuming as the cycling has to be done over several thousand times. Also, in batteries, a simple charge/discharge at several cycles can give valuable insight to the stability of the device. This is because batteries gradually show degradation from the bulk of the electrode material due to charge transfer reactions taking place within (Weingarth *et al.*, 2013). However, EDLCs have the capability of discharging to zero, so carrying out a charge/discharge which is done at voltages far lower than the nominal device voltage will return little or no degradation which leads to wrong conclusion on the device stability.

In EDLCs, charges are stored via electrostatic adsorption-desorption at the interfacial region between the electrodes and the electrolyte under an applied cell voltage. This does not give room for chemical reactions as in the case of batteries and pseudocapacitors which rely on redox reactions. As a result charge transfer is more of a physical process than chemical so it can continue during the charge and discharge process for a lengthy period without noticeable degradation (Šedajová *et al.*, 2020). A more appropriate thing to do will be to expose the device to higher voltage levels. The possibility of increased ionic transfer activities at elevated voltages causing degradation had been proposed (Hahn *et al.*, 2006), though other parameters like the nature of the electrolyte and its gradual degradation at elevated voltage are also of importance when studying the stability status of EDLCs (Ruch *et al.*, 2010). In this study, the constant load or floating test is used, where the capacitor is held at a nominal cell voltage and the capacitance is determined as a function of time. This is considered a more reliable way of testing the stability of supercapacitors since the test is carried out at the highest possible voltage hence can give a clearer insight to future possibilities of degradation as compared to cyclic testing which is done at low voltages especially for activated-carbon based devices hence it reveals no significant degradation after cycling.

In this paper, we investigate a unique synthetic technique for creating hierarchical activated carbon from waste cassava peel, which acts as a precursor in a simple chemical activation method based on potassium bicarbonate

(KHCO₃). In comparison to potassium hydroxide (KOH), which is commonly employed but is severely corrosive to metals and tissues, activating agent (KHCO₃) provides an environmentally benign and secure activation approach. The materials' morphology, structure, surface area, and electrochemical capability were also investigated. Superior electrochemical performances with high specific energy and power densities demonstrated the benefits of KHCO₃ and the good quality of the porous carbon generated using cassava peels precursors via the one-step integrated carbonization/activation process.

MATERIALS AND METHODS

Synthesis of Activated carbon

Cassava peels were washed multiple times to ensure maximum cleanliness. The samples were then dried in an oven at 600 °C for twelve 12 h before being crushed and ball-milled into a fine powder. The sample was combined with potassium bicarbonate (KHCO₃) in a 3:4 ratio using an agate mortar (Amakoromo *et al.*, 2021). The mixture was then carbonized under the flow of Nitrogen gas (N₂) in a Carbolite tube furnace at 750 °C with a ramp rate of 5 °C/min for 1 h. The carbonized material was cooled to room temperature and washed repeatedly with distilled water until a pH of 7 was achieved. The samples were then dried in an oven at 80 °C for 24 h.

Material Characterization

Scanning electron microscopy (SEM) images were studied using a Zeiss EVO/LS10 with an accelerating voltage of 5 kV and with a field emission scanning electron microscope. Nitrogen physisorption experiments were conducted to characterize the Brunauer-Emmett-Teller (BET) specific surface area and pore size distribution. The samples were degassed at 1000°C for 6 h in a vacuum atmosphere. Using a J.Y. Horiba Raman spectrometer with a 15mW power, Raman analysis was performed, whilst X-ray diffraction (XRD) at 2 reflection geometry was used to study the degree of crystallinity and structure of the generated carbon. (Amakoromo *et al.*, 2021).

ELECTROCHEMICAL ANALYSIS

The AC, acetylene black, and polytetrafluoroethylene (PTFE) were mixed in an 8:1:1 mass ratio and then added to ethanol to form a homogeneous slurry that was sprayed onto carbon paper. In a vacuum oven, the sample was dried overnight at 60 °C. The mass loading was 3 mg cm⁻², and the surface area of the working electrode was 1.6 cm².

The symmetric supercapacitor was made consisting of two identical working electrodes, a separator, and 6 M KOH/1 M Na₂SO₄ aqueous electrolytes. The electrochemical characteristics of the samples were measured using cyclic voltammetry (CV), galvanostatic charge discharge (GCD), and electrochemical impedance spectroscopy (EIS) on a BIO-LOGIC (BCS-805) electrochemical working station with the BT-Lab software. EIS was performed at an open circuit voltage of 100 kHz to 0.01 Hz with an AC voltage

amplitude of 5 mV. The cyclic voltammometry (CV) of the setup was investigated at increasing scan rates and voltages. Galvanostatic charge-discharge (GCD) studies were also carried out at various currents and voltages. Ccell (farads) of the symmetric device was computed using galvanostatic cycles (GCD curves), as stated in equation 1..

Where I is the constant current(A), Δt is the charge/discharge time(s) and ΔV, is the change in voltage without the ohmic drop(Ruiz *et al.*, 2009).

While the specific capacitance of a single electrode Celectrode was calculated using equation 2

Where m is the mass (g)of carbon material in a single electrode(Bello *et al.*, n.d.)

The constant voltage hold test otherwise known as the floating test which is an accelerated aging process was carried out to determinate the cell stability still using

$$C_{cell} (F) = I \frac{\Delta t}{\Delta V} \quad (1)$$

the same BIOLOGIC electrochemical workstation. The process involved holding the device for a maximum potentiostatic voltage of 1.6V followed by five galvanostatic discharge (GCD) cycles which were applied

$$C_{electrode} (F g^{-1}) = \frac{4C_{cell}}{m} \quad (2)$$

at a 1Ag-1 of constant current. This procedure was repeatedly continued for 72 h while specific capacitance values were evaluated for every 5h at the 5th discharge cycle.

RESULTS AND DISCUSSION

Fig. 1a shows a schematic representation of the AC preparation process. The mixture was uniformly combined by directly dissolving the crushed casava peel and KHCO₃. KHCO₃ was used as both a foaming template and an etching agent during calcination to create the hierarchical porous structure. Then, the

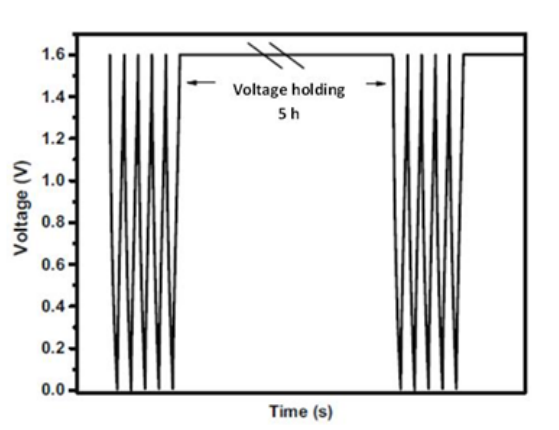


Figure 1: Floating test illustration with 5 charge/discharge cycles at 5 h voltage holding interval.

microstructure of CPC was examined using SEM. The SEM micrograph (Fig1a) depicts a hierarchical porous carbon material with a wrinkled surface and irregular bubbles and defects that has been looped together to produce an interconnected porous structure suitable for effective charge storage. The activated carbon exhibits a wrinkled honeycomb-like morphology, indicating that it is governed by disordered micropores, which is favourable for ion storage and ideal for electrode-electrolyte interactions, as shown in the micrograph. (Vijayakumar *et al.*, 2020). The sample's XRD patterns are depicted in Fig. 1b. The samples exhibit two large distinctive peaks at 23° and 43° , which correspond to the (002) and (100) graphitic carbon planes, respectively. It also displays the incomplete stacking structure of graphite. Graphitic lattice was disrupted by KHCO_3 during calcination of AC samples, preventing the formation of unique long-range ordered graphitic carbon. (Xie *et al.*, 2020). Fig. 1c depicts the Raman spectra of activated carbon, which exhibits a D band at 1357cm^{-1} and a G band at 1582cm^{-1} . Where D is the diamond phase of carbon and G is its graphitic phase. The D-band corresponds to sp^3 -type disordered carbon and defect sites, while the G-band corresponds to sp^2 -type graphitic carbon. The relative intensity (ID/IG) is used to determine the degree of defects and disorder in carbon materials. A lower ID/IG ratio suggests a greater degree of graphitization. The estimated value of AC is 0.85, indicating the degree of

graphitization of AC. (Zequine *et al.*, n.d.).

Another key aspect in determining the capacitance performance of carbon materials is their porous structure. Fig. 1d depicts the N_2 adsorption-desorption isotherms and pore size distributions (inset) of the AC sample. The reversibility of the adsorption-desorption isotherms demonstrates the presence of prominent micropores with a good network. The fast increase at low relative pressure (P/P_0 0.02) shows huge micropores, whereas the big type-H4 hysteresis loops at $P/P_0=0.45-1.0$ and the continued increase at $P/P_0=1.0$ exhibit co-existence, indicating that micropores and mesopores coexist (Amakoromo *et al.*, 2021). The specific surface area (SSA) of the sample was measured using the BET model, and a value of $586\text{m}^2\text{g}^{-1}$ was obtained. Pore size is concentrated between 0.5 and 5 nm. Clearly, the increased specific surface area and the presence of hierarchical pores will enable AC to have more active sites for ion adsorption/desorption, hence improving the capacitance performance.

To evaluate the electrochemical performance of the electrode material, a two electrode setup was done in a 1M Na_2SO_4 electrolyte solution at an optimum voltage of 1.6V. The electrochemical results obtained are presented in Fig. 2.

To evaluate the practical use, the symmetric SC was assembled using AC as both positive and negative

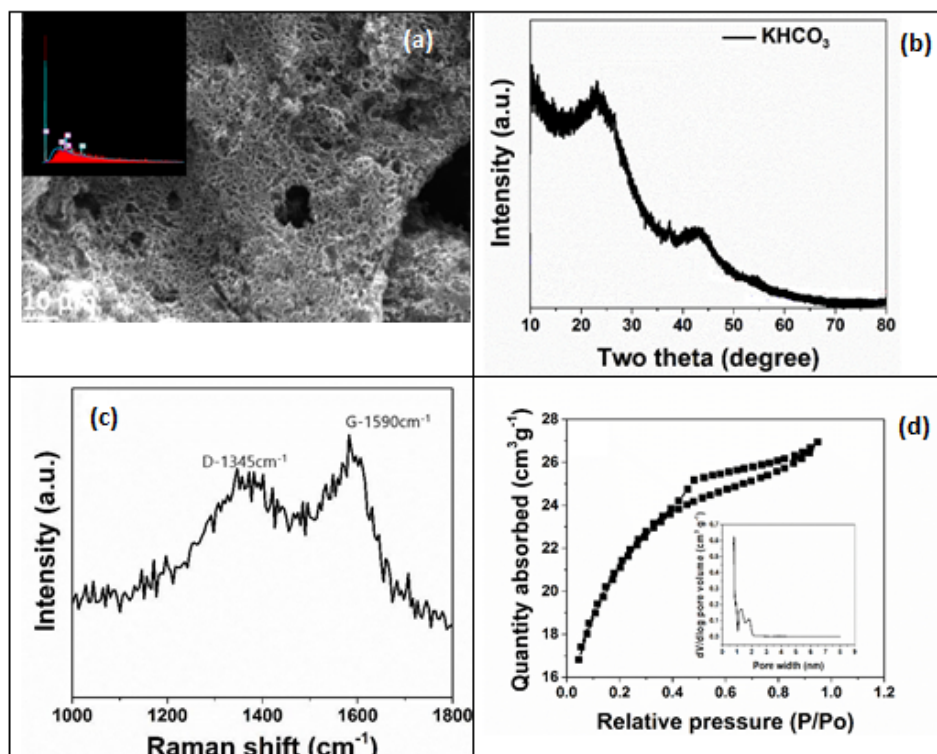


Figure 1: (a) Scanning electron micrograph for KHCO_3 activated carbon (b) Gas adsorption/desorption isotherms of the carbon (c) Raman spectrum of the carbon material (d) XRD of the activated carbon.

electrodes and 1 M Na_2SO_4 as electrolyte. Figure 2(a) illustrates the cyclic voltamogram between 1.0V and 1.6V. The device displayed stability even at 1.6V, as evidenced by its quasi-rectangular shape, which is indicative of

a dominating double layer mechanism [9] and its low resistance, which can be attributed to contributions from the employed aqueous electrolyte (Na_2SO_4) as a high conducting medium [28]. Figure 2(b) demonstrates that

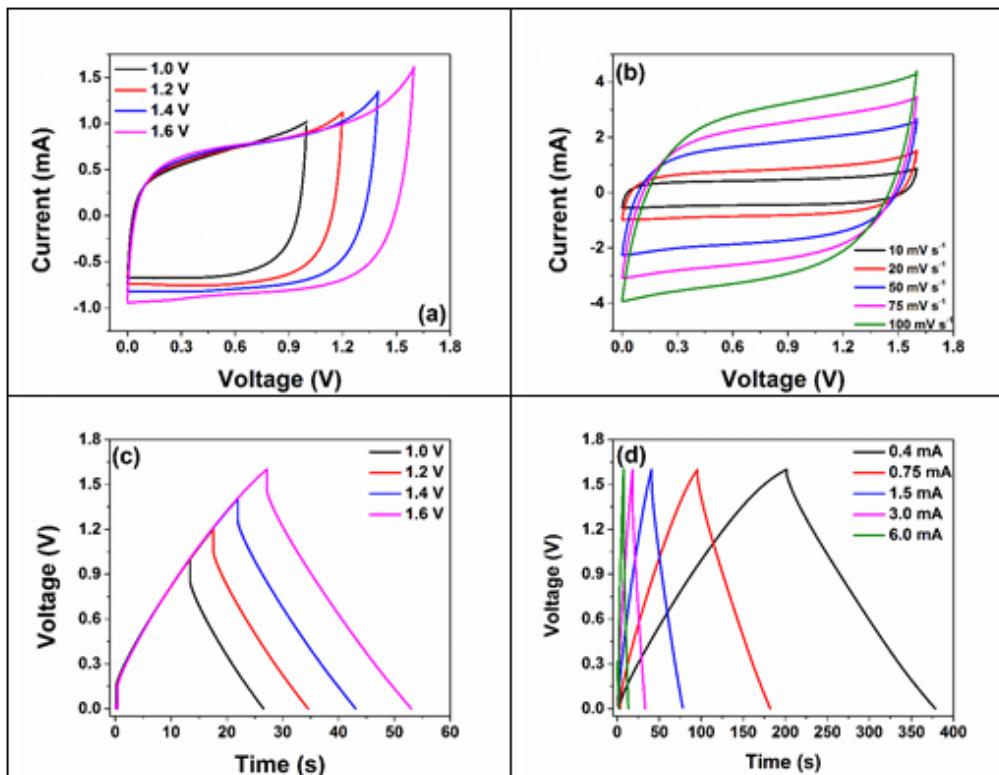


Figure 2: (a) CV at different voltage from 1.0 -1.6 V (b) CV at different scan rates from 10- 100 mV s⁻¹ (c) GCD at 2 mA for different voltages from 1.0 -1.6 V (d) GCD at different current from 0.4 – 6 mA.

as the scan rate increases from 10 to 100mVs⁻¹, the CV curves approach a rectangular shape, indicating that the electrode material has an excellent rate capacity. At a scan rate of 100mVs⁻¹, however, it begins to assume a near-oval shape, indicating that the device begins to become resistive. The CV curves of AC SC maintain comparable quasi-rectangular forms as the scan rate increases from 10 to 100 mV s⁻¹, indicating outstanding rate performance and quick charge transfer kinetics.

The GCD curves are practically linear and show symmetrical triangular shapes in the range 2mA and different voltages (1V to 1.6V), confirming the typical EDLC properties and great reversibility (Fig. 2c). There is no visible IR drop at the beginning of the discharge, and the GCD curves exhibit a nearly symmetric triangular shape with negligible ohmic drops, even as the voltage is increased, indicating high electrochemical reversibility and a solid EDL charge storage mechanism. At 1.6V, the GCD was executed at various particular currents. From the discharge curves, the specific capacitance of the cell was calculated using equation (1). Additionally, the long-term stability is another determining factor for high performance SCs. Figure 3(a) shows the specific capacitance of the cell with a value of 55Fg⁻¹ at specific current of 0.1 Ag⁻¹ and 35 Fg⁻¹ at 1.5 Ag⁻¹ specific current this shows a loss of about 36% when exposed to a higher current density, confirming an excellent rate capability. The energy and power characteristics of the device, when presented in Ragone plot (Figure 3(b)), presents a stable energy density of the device even at

higher power densities. The Ragone plot is shown in Fig. 3b, indicates that SC delivers the maximum energy density of 8.14 Wh kg⁻¹ at a power density of 250 W kg⁻¹. The result is indicative of a device with high rate capability and shows properties of carbon electrode material with highly porous characteristics. The voltage hold (floating) test, an accelerated aging process was utilized as a stability test for the device. This method offers a more practical approach in testing the stability of the device than subjecting it to several thousand cycles. A 10h floating period is followed by consecutive constant current charge discharge (CCCD) cycles to identify any capacitance loss over a 72 h (3days) period. Figure 3c shows the gradual regression in cell capacitance over the 72 h floating period. It was observed that within the first 50 h, there was no noticeable loss in capacitance which shows high stability at the set voltage of 1.6V and time window. However, beyond 50hrs exposure and running upto 72 h, a capacitance loss of 44% was observed. Figure 3d shows the self-discharge cycle of the cell. While emphasis has been placed on enhancing supercapacitor energy and power densities, little attention has been paid to hybrid supercapacitor self-discharge. Self-discharge is the voltage drop that occurs naturally in energy storage devices after a period of storage, leading to the loss of stored energy. (Self-Discharge of Electrochemical Double Layer Capacitors - Physical Chemistry Chemical Physics (RSC Publishing), n.d.) The majority of the battery's energy is stored in the electrodes, resulting in a gradual self-discharge. The substantially quicker self-discharge

rate observed in electrical double-layer capacitors is typically attributed to the electrostatic adsorption of ions at the electrode/electrolyte interface. This device's self-discharge phenomenon was intensively examined because it poses a significant threat to the mainstream use of supercapacitors. A low current density of 0.1 Ag⁻¹ was used to charge the cell to a specified voltage, and it was maintained for 30 minutes to ensure the SC stayed fully charged. The self-discharge voltage curves for various starting voltages are depicted in Figure 3d.

The initial voltage has a significant effect on the rate of self discharge, which is defined by the Gibbs energy minimization of the system. (Conway *et al.*, 1997) Due to the fact that 75% of a supercapacitor's stored energy is lost when its voltage falls to half of its original voltage, a rapid voltage drop can severely degrade a supercapacitor's functionality (Andreas, 2015). According to Chen *et al.* (Chen *et al.*, 2014) the rapid drop in cell voltage during the initial stage of self-discharge is likely owing to the

decomposition of the solvent, which in this case is water. Briefly, the solvent can be abridged on the cathode when the gadget is totally charged. This drop can continue even after the current is stopped, resulting in a rapid decrease in cathode potential. This process is affected by the surface quality of the electrode and is neither diffusion-controlled nor current-leakage-controlled. Consequently, any analysis of the self-discharge mechanism will omit this potential drop.

The device retains its original rectangular shape even when the capacitance decreases slightly, as seen in Fig. 4a. The modest deviation from rectangular behavior is due to proton electrosorption on the nanostructure surfaces. Possible sources include the functional groups on the surface and the carbon material itself. The comparison CVs show that the electrodes of the symmetric device show negligible degradation following a voltage holding or floating test (aging).

Figure 4b shows the Nyquist plot of the device's

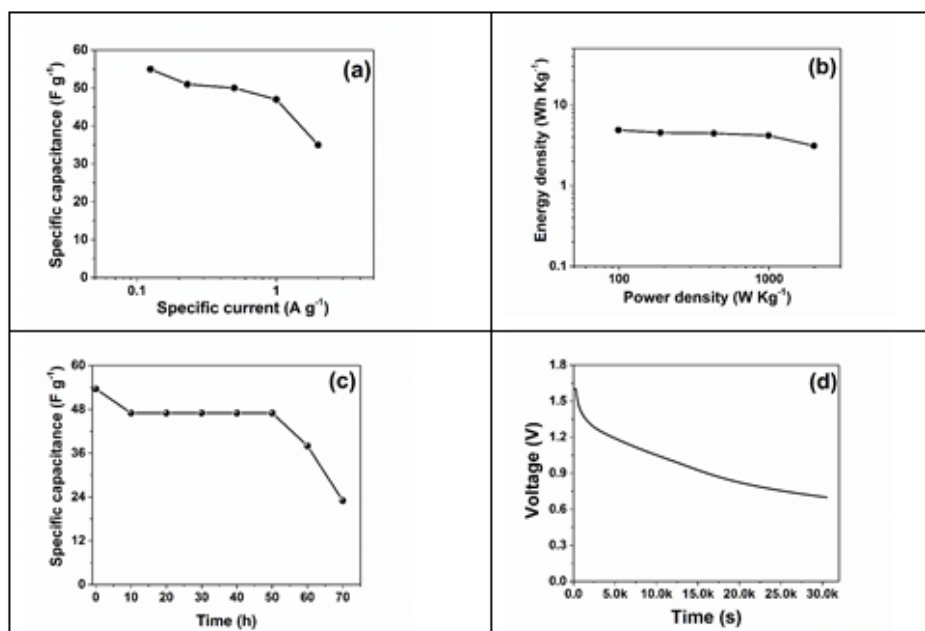


Figure 3: (a) Specific capacitance as a function of the specific current (b) Ragone plot (c) floating test for 72 hr and (d) self-discharge of the device.

electrochemical impedance spectroscopy (EIS), both pre- and post-floating. Similar internal resistance values (ESR) in the Nyquist plots before and after floating reveal that the floating test has no effect on the device..

To investigate the frequency behavior and calculate the relaxation time constant of porous electrodes (Taberna *et al.*, 2003), a complex capacitance model based on a

single RC time-constant was used to define both the real portion C' (ω) and the imaginary part C'' (ω) capacitance as a function of frequency. The results demonstrate that porous carbon has a quick frequency response, superior power delivery, and high capacitance and retention. This dispersion of energy is depicted by the blue curve, which is the capacitance's imaginary component. The

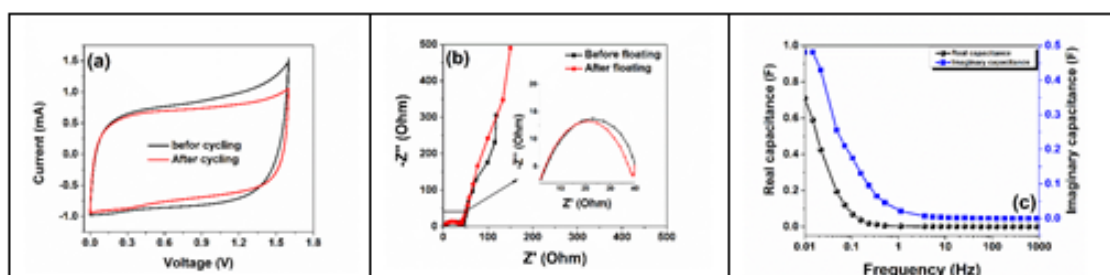


Figure 4: (a) CV stability test and (b) EIS measurement before and after cycling (c) imaginary and real capacitance as a function of the frequency.

time between the capacitive and resistive behavior of the supercapacitor electrode 46 was used to compute the relaxation time (τ), which calculated from $\tau=1/\omega_{\max}=1/(2\pi f_{\max})$ where f_{\max} is the characteristic frequency of the cell obtained at the phase angle of -45° . The calculated relaxation duration of 9.5 seconds indicates that the accumulated energy can be properly discharged within this timeframe.

CONCLUSION

Activated carbon with specific surface area of 586m²g⁻¹ was synthesized from cassava peels waste using KHCO₃. The produced electrodes in a neutral electrolyte (Na₂SO₄) showed good electrochemical performance and stability. The assembled symmetric device, gave a specific capacitance of 55Fg⁻¹ at 0.1Ag⁻¹. The device showed a near insignificant capacitance loss when exposed to accelerated aging through a floating test. These results show that further enhancement on the material shows great promise for production of stable supercapacitor devices.

REFERENCE

- Amakoromo, T. E., Abumere, O. E., Amusan, J. A., Anye, V., & Bello, A. (2021). Porous Carbon from Manihot Esculenta (Cassava) Peels Waste for Charge Storage Applications. *Current Research in Green and Sustainable Chemistry*, 4(March), 100098. <https://doi.org/10.1016/j.crgsc.2021.100098>
- Andreas, H. A. (2015). Self-Discharge in Electrochemical Capacitors: A Perspective Article. *Journal of The Electrochemical Society*, 162(5), A5047–A5053. <https://doi.org/10.1149/2.0081505jes>
- Bello, A., Barzegar, F., Madito, M. J., Momodu, D. Y., Khaleed, A. A., Masikhwa, T. M., Dangbegnon, J. K., & Manyala, N. (n.d.). *Stability studies of polypyrrole-derived carbon based symmetric supercapacitor via potentiostatic floating test.*
- Bello, A., Barzegar, F., Madito, M. J., Momodu, D. Y., Khaleed, A. A., Masikhwa, T. M., Dangbegnon, J. K., & Manyala, N. (2016). Stability studies of polypyrrole-derived carbon based symmetric supercapacitor via potentiostatic floating test. *Electrochimica Acta*, 213, 107–114. <https://doi.org/10.1016/j.electacta.2016.06.151>
- Chen, L., Bai, H., Huang, Z., & Li, L. (2014). Mechanism investigation and suppression of self-discharge in active electrolyte enhanced supercapacitors. *Energy & Environmental Science*, 7(5), 1750–1759. <https://doi.org/10.1039/c4ee00002a>
- Conway, B. E., Pell, W. G., & Liu, T. C. (1997). Diagnostic analyses for mechanisms of self-discharge of electrochemical capacitors and batteries. *Journal of Power Sources*, 65(1–2), 53–59. [https://doi.org/10.1016/S0378-7753\(97\)02468-3](https://doi.org/10.1016/S0378-7753(97)02468-3)
- Electrochemical Capacitive Performance of ZnCl₂ Activated Carbon Derived from Bamboo Bagasse in Aqueous and Organic Electrolyte : *Oriental Journal of Chemistry*. (n.d.). Retrieved January 30, 2023, from <http://www.orientjchem.org/vol35no1/electrochemical-capacitive-performance-of-zncl2-activated-carbon-derived-from-bamboo-bagasse-in-aqueous-and-organic-electrolyte/>
- Elgendy, A., El Basiony, N. M., El-Taib Heakal, F., & Elkholy, A. E. (2020). Mesoporous Ni-Zn-Fe layered double hydroxide as an efficient binder-free electrode active material for high-performance supercapacitors. *Journal of Power Sources*, 466(32), 228294. <https://doi.org/10.1016/j.jpowsour.2020.228294>
- Hahn, M., Barbieri, O., Campana, F. P., Kötzt, R., & Gally, R. (2006). Carbon based double layer capacitors with aprotic electrolyte solutions: The possible role of intercalation/insertion processes. *Applied Physics A: Materials Science and Processing*, 82(4 SPEC. ISS.), 633–638. <https://doi.org/10.1007/s00339-005-3403-1>
- Huang, Y., He, J., Luan, Y., Jiang, Y., Guo, S., Zhang, X., Tian, C., & Jiang, B. (2017). Promising biomass-derived hierarchical porous carbon material for high performance supercapacitor. *RSC Advances*, 7(17), 10385–10390. <https://doi.org/10.1039/C6RA27788H>
- Jin, H., Wang, X., Gu, Z., Hoefelmeyer, J. D., Muthukumarappan, K., & Julson, J. (2014). Graphitized activated carbon based on big bluestem as an electrode for supercapacitors. *RSC Advances*, 4(27), 14136–14142. <https://doi.org/10.1039/c3ra46037a>
- Jo, S., Jayababu, N., & Kim, D. (2022). Rational design of cobalt-iron bimetal layered hydroxide on conductive fabric as a flexible battery-type electrode for enhancing the performance of hybrid supercapacitor. *Journal of Alloys and Compounds*, 904, 164082. <https://doi.org/10.1016/j.jallcom.2022.164082>
- Li, G., Li, Y., Chen, X., Hou, X., Lin, H., & Jia, L. (2022). One step synthesis of N, P co-doped hierarchical porous carbon nanosheets derived from pomelo peel for high performance supercapacitors. *Journal of Colloid and Interface Science*, 605, 71–81. <https://doi.org/10.1016/j.jcis.2021.07.065>
- Ma, X., Yang, H., Yu, L., Chen, Y., & Li, Y. (2014). Preparation, surface and pore structure of high surface area activated carbon fibers from bamboo by steam activation. *Materials*, 7(6), 4431–4441. <https://doi.org/10.3390/ma7064431>
- Moyo, B., Momodu, D., Fasakin, O., Dangbegnon, J., & Manyala, N. (1911). Electrochemical analysis of nanoporous carbons derived from activation of polypyrrole for stable supercapacitors. *Journal of Materials Science*. <https://doi.org/10.1007/s10853-017-1911-y>
- Mutuma, B. K., Sylla, N. F., Bubu, A., Ndiaye, N. M., Santoro, C., Brilloni, A., Poli, F., Manyala, N., & Soavi, F. (2021). Valorization of biodigester plant waste in electrodes for supercapacitors and microbial fuel cells. *Electrochimica Acta*, 391, 138960. <https://doi.org/10.1016/j.electacta.2021.138960>
- Noori, A., El-Kady, M. F., Rahmanifar, M. S., Kaner, R. B.,

- & Mousavi, M. F. (2019). Towards establishing standard performance metrics for batteries, supercapacitors and beyond. *Chemical Society Reviews*, 48(5), 1272–1341. <https://doi.org/10.1039/c8cs00581h>
- Nwabanne, & Igbokwe P. K. (2011). Preparation of Activated Carbon from Nipa Palm Nut: Influence of Preparation Conditions. *In Research Journal of Chemical Sciences* (Vol. 1, Number 6).
- Ruch, P. W., Cericola, D., Foelske-Schmitz, A., Kötz, R., & Wokaun, A. (2010). Aging of electrochemical double layer capacitors with acetonitrile-based electrolyte at elevated voltages. *Electrochimica Acta*, 55(15), 4412–4420. <https://doi.org/10.1016/j.electacta.2010.02.064>
- Ruiz, V., Santamaría, R., Granda, M., & Blanco, C. (2009). Long-term cycling of carbon-based supercapacitors in aqueous media. *Electrochimica Acta*, 54(19), 4481–4486. <https://doi.org/10.1016/j.electacta.2009.03.024>
- Šedajová, V., Jakubec, P., Bakandritsos, A., Ranc, V., & Otyepka, M. (2020). New limits for stability of supercapacitor electrode material based on graphene derivative. *Nanomaterials*, 10(9), 1–14. <https://doi.org/10.3390/nano10091731>
- Self-discharge of electrochemical double layer capacitors - Physical Chemistry Chemical Physics (RSC Publishing). (n.d.). Retrieved February 28, 2026, from <https://pubs.rsc.org/en/content/articlelanding/2013/cp/c3cp44612c>
- Sevilla, M., & Fuertes, A. B. (n.d.). *green approach supercapacitor electrodes : chemical activation of hydrochar with potassium bicarbonate*. 1–31.
- Sevilla, M., & Fuertes, A. B. (2016). *A Green Approach to High-Performance Supercapacitor Electrodes : The Chemical Activation of Hydrochar with Potassium Bicarbonate*. 1–10. <https://doi.org/10.1002/cssc.201600426>
- Sevilla, M., & Mokaya, R. (n.d.). *Energy storage applications of activated carbons supercapacitors and hydrogen storage - Energy & Environmental Science* (RSC Publishing).
- Taberna, P. L., Simon, P., & Fauvarque, J.-F. (2003). Electrochemical characteristics and impedance spectroscopy studies of carbon-carbon supercapacitors. *Journal of The Electrochemical Society*, 150(3), A292–A300.
- Vijayakumar, M., Bharathi Sankar, A., Sri Rohita, D., Nanaji, K., Narasinga Rao, T., & Karthik, M. (2020). Achieving High Voltage and Excellent Rate Capability Supercapacitor Electrodes Derived From Bio-renewable and Sustainable Resource. *ChemistrySelect*, 5(28), 8759–8772. <https://doi.org/10.1002/slct.202001877>
- Weingarth, D., Foelske-Schmitz, A., & Kötz, R. (2013). Cycle versus voltage hold - Which is the better stability test for electrochemical double layer capacitors? *Journal of Power Sources*, 225, 84–88. <https://doi.org/10.1016/j.jpowsour.2012.10.019>
- Xie, X. B., Wu, D., Wu, H., Hou, C., Sun, X., Zhang, Y., Yu, R., Zhang, S., Wang, B., & Du, W. (2020). Dielectric parameters of activated carbon derived from rosewood and corncob. *Journal of Materials Science: Materials in Electronics*, 31(20), 18077–18084. <https://doi.org/10.1007/s10854-020-04358-8>
- Yakout, S. M., & Sharaf El-Deen, G. (2016). Characterization of activated carbon prepared by phosphoric acid activation of olive stones. *Arabian Journal of Chemistry*, 9, S1155–S1162. <https://doi.org/10.1016/j.arabjc.2011.12.002>
- Yang, S., & Zhang, K. (2018). Converting Corncob to Activated Porous Carbon for Supercapacitor Application. *Nanomaterials*, 8(4), 181. <https://doi.org/10.3390/nano8040181>
- Zequine, C., Ranaweera, C. K., Wang, Z., Dvornic, P. R., Kahol, P. K., Singh, S., Tripathi, P., Srivastava, O. N., Singh, S., Kumar Gupta, B., Gupta, G., & Gupta, R. K. (n.d.). *High-Performance Flexible Supercapacitors obtained via Recycled Jute: Bio-Waste to Energy Storage Approach OPEN*. <https://doi.org/10.1038/s41598-017-01319-w>
- Zhu, X., Huang, X., Anwer, S., Wang, N., & Zhang, L. (2020). Nitrogen-Doped Porous Carbon Nanospheres Activated under Low ZnCl₂Aqueous System: An Electrode for Supercapacitor Applications. *Langmuir*, 36(31), 9284–9290. https://doi.org/10.1021/ACS.LANGMUIR.0C01670/SUPPL_FILE/LA0C01670_SI_001.PDF
- ZINC chloride | ZnCl₂ - PubChem. (n.d.). Retrieved January 30, 2023, from <https://pubchem.ncbi.nlm.nih.gov/compound/ZINC-chloride>